第 28 卷第 11 期
2012 年 11 月

无 机 化 学 学 报
CHINESE JOURNAL OF INORGANIC CHEMISTRY

Vol.28 No.11
2401-2406

电泳法制备具有{001}面 TiO_2 纳米片分级球散射层的染敏太阳电池光电极

唐泽坤[1,2] 黄 欢[1,2] 管 杰[1,2] 于 涛*[,1,2] 邹志刚[1,3]

([1]南京大学固体微结构物理国家重点实验室,南京 210093)

([2]南京大学物理学院环境材料与再生能源研究中心,南京 210093)

([3]南京大学材料科学与工程系,南京 210093)

摘要: 利用简便的溶剂热法,制得了由锐钛矿相的纳米片组成的、{001}面接近 100%暴露的 TiO_2 分级球形结构。利用电泳沉积法,将所得的 TiO_2 分级球形结构作为散射层引入到染料敏化太阳电池(DSSC)中,并很好地保护了这种脆弱的分级结构。由于这种分级球形结构比 TiO_2 纳米颗粒具有更好的染料吸附性能和光散射性能,使用这种 TiO_2 分级球形结构作为散射层的 DSSC 达到了 7.38%的光电转换效率,较之基于 TiO_2 纳米颗粒的 DSSC 有了 26%的提高。

关键词: 染料敏化太阳电池; {001}面 TiO_2 分级球; 散射层; 电泳沉积

中图分类号: O614.41$^+$1; TM914.4$^+$2 **文献标识码**: A **文章编号**: 1001-4861(2012)11-2401-06

Dye-Sensitized Solar Cells with An Electrophoresis-Deposited Layer of {001} Exposed Nanosheet-Based Hierarchical TiO_2 Spheres

TANG Ze-Kun[1,2] HUANG Huan[1,2] GUAN Jie[1,2] YU Tao*[,1,2] ZOU Zhi-Gang[1,3]

([1]*National Laboratory of Solid State Microstructures, Nanjing University, Nanjing* 210093, *China*)

([2]*Eco-materials and Renewable Energy Research Center , Department of Physics, Nanjing University, Nanjing* 210093, *China*)

([3]*Department of Materials Science and Engineering, Nanjing University, Nanjing* 210093, *China*)

Abstract: Anatase TiO_2 nanosheet-based hierarchical spheres (HSs) with nearly 100% exposed {001} facets were synthesized via a facile solvothermal process. Using these hierarchical spheres as a scattering layer on nanocrystaline TiO_2 film, bi-layered dye-sensitized solar cells (DSSCs) have been fabricated by electrophoresis deposition method, which well preserved the fragile hierarchical structure. Owing to the superior dye adsorption and light scattering effect of HSs, an overall energy conversion efficiency of 7.38% is achieved, which is 26% higher than that of nanoparticle-based photoanode.

Key words: dye-sensitized solar cells; {001} exposed TiO_2 hierarchical sphere; scattering layer; electrophoresis deposition

Dye sensitized solar cells (DSSCs) have been studied extensively since O′Regan and Grätzel′s outstanding breakthrough in 1991, and unprecedented efficiency of 12.3% achieved very recently has further encouraged the researchers′ interests[1-2]. Harboring the advantages of relatively high efficiency, nontoxicity and low cost, DSSC stands out as a promising candidate to solve the increasingly serious energy crisis. The core part of a DSSC is a dye-coated semiconductor (mostly TiO_2) thin film, where the dye

收稿日期:2012-03-20。收修改稿日期:2012-05-10。

国家自然科学基金(No.11174129)、江苏省自然科学基金(BK2011056)、中央高校基本科研业务费专项资金(1116020406)资助项目。

*通讯联系人。E-mail:yutao@nju.edu.cn; 会员登记号:S02P210167M 。

molecules harvest and utilize the sunlight. For a conventional efficient TiO_2-based DSSC, small nanoparticles (10~30 nm) with large surface area for dye adsorption are required, while the resulting photoanode usually exhibits high transparency and therefore causes a considerable transmittance of light[3-5]. Meanwhile, the mostly used dyes (N719, N3) show a fairly poor absorption of sunlight in the range of long wavelength. These unfavorable characters of dye-coated photoanode lead to an unsatisfying harvesting of the sunlight. Enhancing the light harvesting efficiency is believed to bear the responsibility for further advancing the performance of DSSCs[6-7]. To this end, incorporating large particles into the nanocrystalline photoanode or depositing a layer of large particles on top of the nanocrystalline photoanode have been proved to be effective ways[8]. However, the introduction of large particles into the photoanode will limit the cell efficiency on account of the insufficient surface area and correspondingly decreased dye adsorption. One strategy to solve this problem is to use a substitute of hierarchically structured large TiO_2 particles. The hierarchical structure permits effective dye-uptake profiting from constituent nano-crystallites while still functions as the scattering layer by the aid of secondary particles. A marked improvement in cell efficiency has been achieved by depositing a scattering layer composed of mesoporous TiO_2 beads[9].

{001} facets exposed anatase TiO_2 crystals possess a larger amount of exposed Ti sites and thus an expected higher dye adsorption[10-12]. Recently Chen et al. reported an anatase nanosheet-based hierarchical spheres with nearly 100% exposed {001} facets[13]. With the expected higher dye adsorption, this unique structure can be an ideal candidate as scatters in the photoanode. Yang et al. reported a 43% increase in energy conversion efficiency by introducing a similar structure as scatters[14]. On the other hand, electrophoresis deposition (EPD) emerges as an effective route to the fabrication of TiO_2 nanocrystalline film, due to its favorable characteristics of low cost, simple equipment, formation of uniform layers with controllable thickness and applicability to nonplanar even complex multi-dimensional substrates[15-16]. Besides, the biggest advantage of EPD is its good repeatability with less demand for skills, which is highly desired for DSSC fabrication. In the case of hierarchical structure, EPD shows superiority in preserving the desirable hierarchical structure in comparison with widely used doctor blading method, which requires a harsh grinding procedure during the preparation of photoanode.

Based on the above consideration, we fabricated a TiO_2 thin film consisting TiO_2 hierarchical spheres with exposed {001} facets as the scattering layer by EPD method. Facilitated by the increased dye adsorption and light harvesting efficiency, a 7.38% overall energy conversion efficiency has been achieved, indicating a 26% increase compared to nanoparticle photoanode (5.87%). This drastic improvement in efficiency suggests that EPD and this newly hierarchical TiO_2 scattering layer are strong tools for further optimization of DSSCs.

1 Experimental

1.1 Preparation of anatase TiO_2 nanosheet-based hierarchical spheres (HSs)

HSs with nearly 100% exposed {001} facets were synthesized according to the previous report[13]. In a typical run, 0.03 mL diethylenetriamine (DETA; 98%, TCI) was added to 42 mL isopropyl alcohol (IPA; 99%, Nanjing Chemical Reagent Ltd.) under gently stirring. After a few minutes, 1.5 mL titanium (IV) isopropoxide (TIP; 98%, Acros Organics) was added. The reaction solution was then transferred to a 60 mL Teflon-lined stainless steel autoclave for solvothermal treatment at 200 ℃ for 24 h. Following this step, the obtained white precipitate was centrifuged and washed thoroughly with ethanol, and then dried at 60 ℃ overnight. Finally, the products were calcined at 400 ℃ for 2 h (ramp rate: 1 ℃·min^{-1}) to obtain a highly crystalline anatase phase.

1.2 Preparation of TiO_2 nanoparticles (NPs)

The TiO_2 nanoparticles were prepared as follows:

6.8 g Tetra-n-butyl Titanate (98%, Nanjing Chemical Reagent Ltd.) was dissolved into 20 mL ethanol and then added to a solution containing 20 mL ethanol, 4 mL water and 4 g acetic acid under stirring. After a thorough hydrolysis for about two hours, the white colloidal sol was transferred to a 60 mL Teflon-lined stainless steel autoclave and kept in an electric oven at 180 ℃ for 20 h. The obtained white precipitate was then harvested and washed with ethanol, and then dried at 60 ℃ for 24 h.

1.3 Fabrication of dye-sensitized solar cells

Fluorine-doped tin oxide (FTO) conductive glass (15 Ω/□) was cleaned by ultrasonic washing before using. The electrophoretic suspension consisted of 50 mL acetone, 10 mg iodine and 40 mg TiO_2, which went through an ultrasonic dispersion before use. For the electrophoresis experiment, two pieces of FTO were used as the anode and cathode and then placed parallel in the electrophoretic suspension, with a distance of 10 mm between them. The EPD voltage was set to 20 V and held for various time to get different film thicknesses. The as prepared film was then heat treated at 500 ℃ for half an hour (ramp rate: 10 ℃ $\cdot min^{-1}$). To enhance the mechanical strength of the film, a half hour treatment of 40 mmol $\cdot L^{-1}$ $TiCl_4$ at 70 ℃ was then performed, followed by another heat treatment at 500 ℃ for 0.5 h. The sintered electrode were immersed in a 3×10^{-4} mol $\cdot L^{-1}$ solution of N719 (Solaronix S.A., Aubonne, Switzerland) in ethanol at room temperature for 24 h. The counter electrode was a magnetron sputter platinum mirror. The substrate, film, and counter electrode constituted a sandwich-like open cell. The electrolyte was composed of 1.0 mol $\cdot L^{-1}$ BMII, 50 m mol $\cdot L^{-1}$ LiI, 30 m mol $\cdot L^{-1}$ I_2, and 0.5 mol $\cdot L^{-1}$ tert-butylpyridine in a mixed solvent of acetonitrile and valeronitrile (85∶15, *V*/*V*).

1.4 Characterizations

X-ray diffraction (XRD) patterns were collected on a Rigaku Ultimal III X-ray diffractometer (Cu $K\alpha$, λ=0.154 18 nm) in the range of 10°~80° at a scan rate of (2θ)0.02° $\cdot s^{-1}$. The applied current and the accelerating voltage were 40 mA and 40 kV, respectively. The BET surface area was measured on a Tristar micromeritics surface area and porosity analyzer. Field-emission scanning electron microscope (FE-SEM) images were characterized on a FEI NANOSEM 230 under an accelerating voltage of 15 kV. The film thickness was measured on a Dektak 6M stylus profiler. The reflectance spectra were tested by a SHIMADZU UV-2550 UV-Visible spectrophotometer. A Cary 50 probe UV-Visible spectrophotometer was used to measure the transmission spectra and UV/Vis absorbance spectra. The test for photoelectric performance was carried out, with an active area of 0.132 cm^2, on a Keithley 236 source measurement unit under AM 1.5 illumination cast by an Oriel 92251A-1000 sunlight simulator calibrated by the standard reference of a Newport 91150 silicon solar cell.

2 Results and discussion

2.1 Characterization analysis

2.1.1 XRD analysis

The crystal structures of NPs and HSs were examined by X-ray diffraction (XRD) analysis (shown in Fig.1), and all of the identified peaks can be indexed to anatase TiO_2 (PDF No. 21-1272), which has been demonstrated suitable for DSSCs[17].

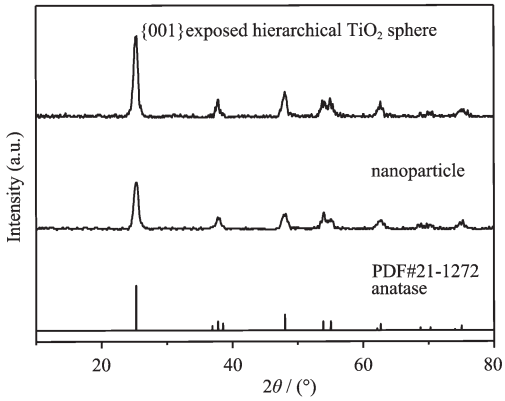

Fig.1 XRD patterns for the as-synthesized HSs and NPs

2.1.2 SEM analysis

The morphology of the as-obtained HSs and NPs were further characterized by SEM. The NPs with an average diameter of 10~20 nm are slightly aggregated as shown in Fig.2a. Fig.2b gives an enlarged picture

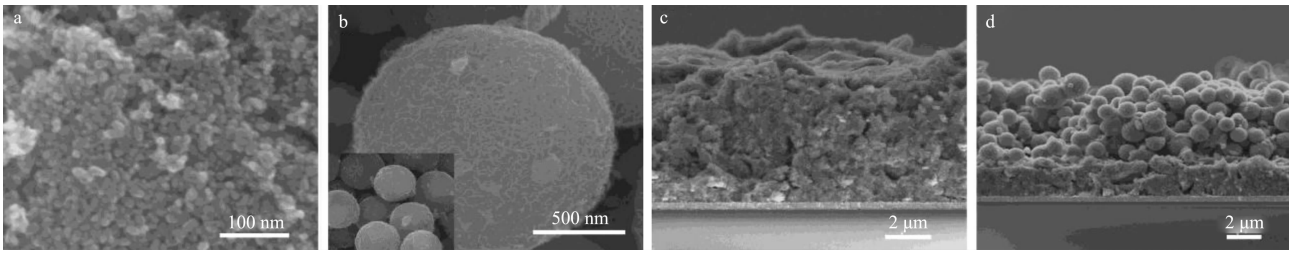

The inset shows HSs in a larger scale; Cross-section images of films composed of NPs and HSs+NPs with a thickness of 9.0 μm (c and d)

Fig.2 FE-SEM images of the as-synthesized NPs and HSs (a and b)

of a single HS, revealing that the HS is built by curved flakes, and the flakes have previously been proved to be bounded by {001} facets on both the top and bottom [13]. The inset in Fig.2b depicts that the obtained spheres are uniform with an average size of 1 μm, which are in good accordance with the previous report[13].

2.1.3 BET surface area analysis

The specific BET surface area of the NPs and HSs are 127 and 114 $m^2 \cdot g^{-1}$, respectively, obtained from the N_2 adsorption-desorption. The N_2 adsorption/desorption isotherm and pore size distribution of the HSs is shown in Fig.3. It gives a sharp capillary condensation step at high relative pressure (P/P_0=0.6~1.0), indicating a mesoporous structure [18]. According to the Barrett-Joyner-Halenda (BJH) model, the inset figure signifies a relative narrow pore size distribution in the range of 5~15 nm for the hierarchical material.

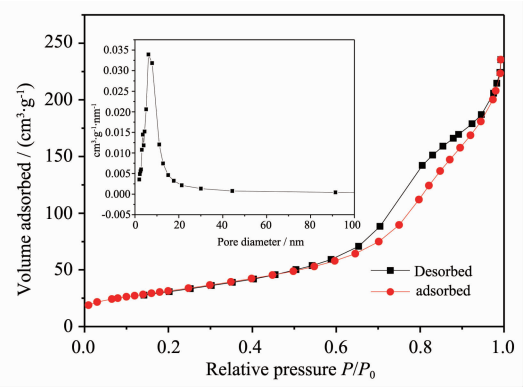

Inset: the pore size distribution of HSs

Fig.3 Nitrogen sorption isotherms of the HSs

2.2 Photovoltaic performance test

The as-prepared HSs and NPs were further used as photoanodes in DSSCs. For comparison, two kinds of films (a: HSs+NPs, b: NPs) with different thicknesses (6.5 μm and 9.0 μm) were fabricated by EPD. To prepare the HSs+NPs film, a layer of NPs was firstly electrophoresis-deposited. After sintered at 450 ℃ for 0.5 h, then an electrophoresis deposition of HSs was followed. The cross-sectional SEM images of NPs film and HSs+NPs film of 9.0 μm are shown in Fig.2c and Fig.2d. Fig.2c indicates a single-layered film of 9.0 μm NPs while Fig. 2d reveals a clear bilayer structure composed of 6.5 μm HSs film and 2.5 μm NPs film. For the 6.5 μm HSs+NPs film, the thicknesses of HSs layer and NPs layer are 4.0 μm and 2.5 μm, respectively. The current density-voltage (*J-V*) curves of the DSSCs based on the two films (cell a: film a; cell b: film b) are shown in Fig.4 and the corresponding cell parameters are listed in Table 1, including the film thickness, open circuit voltage (V_{oc}), short circuit current density (J_{sc}), fill factor (FF), and efficiency (η). As shown in Fig.4 and Table 1, the V_{oc} and FF of the DSSCs based on the two films do not have significant variations. However, for a cell of 6.5 μm, the J_{sc} increases from 11.0 mA·cm^{-2} to 13.1 mA·cm^{-2} as the HSs are introduced,

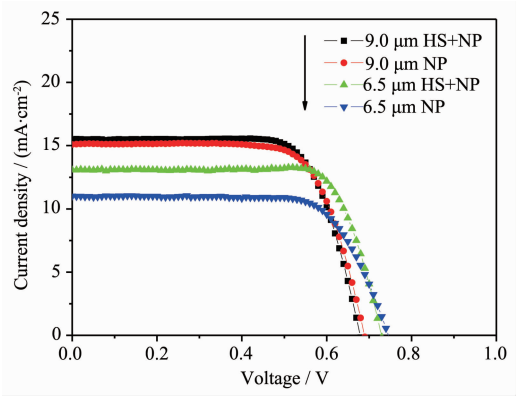

Fig.4 Current density and voltage characteristics of DSSCs under AM 1.5 illumination with an active area of 0.132 cm^2

Table 1　Characteristics of DSSCs based on photoanodes of TiO_2 nanoparticles (NPs) and TiO_2 hierarchical spheres plus TiO_2 nanoparticles (HSs+NPs) with two kinds of film thicknesses

Photoanodes	Thicknesses / μm	V_{oc} / V	J_{sc} / (mA·cm^{-2})	FF / %	η / %
NP 1	6.5	0.74	11.0	71.7	5.87
NP+HT 1	6.5	0.73	13.1	77.6	7.38
NP 2	9.0	0.69	15.1	71.9	7.48
NP+HT 2	9.0	0.68	16.5	73.0	7.66

leading to a η improvement from 5.87% to 7.38%. For a cell of 9.0 μm, the increasement of J_{sc} is not that obvious, slightly from 15.1 mA·cm^{-2} to 16.5 mA·cm^{-2} and resulting in a similar η of 7.48% to 7.66%.

As the photocurrent is strongly related to the dye loading on the TiO_2 photoelectrode [19], the saturation adsorption capacity of N719 dye was therefore measured. The amount of adsorbed dye per unit surface area (desorbed from the electrode by NaOH aqueous solution) for HSs and NPs are 5.37×10^{-7} mol·m^{-2} and 4.66×10^{-7} mol·m^{-2}, respectively. The increase in the dye loading capacity of HSs can be attributed to a relatively large surface area and widely exposed {001} facets, which lead to more photogenerated electrons and higher photocurrents. This is in well agreement with the *J-V* data.

Hierarchical spheres with submicron size consisting of nanoparticles have been proved to enhance the light scattering effect, hence resulting in a higher photocurrent [20]. The reflectance spectra and transmission spectra of these two kinds of cells are further characterized and shown in Fig.5 and Fig.6. The reflectance for a bi-layered cell consisting HSs as

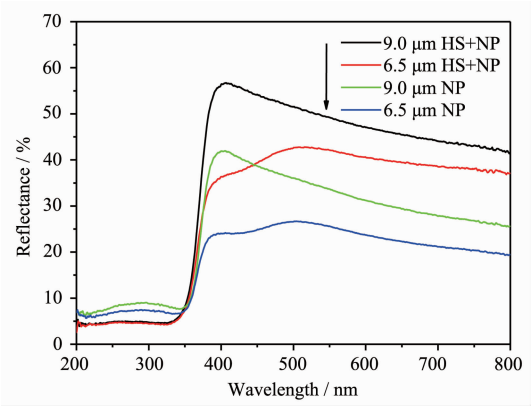

Fig.5　Diffuse reflectance spectra of two kinds of electrode films with similar thicknesses

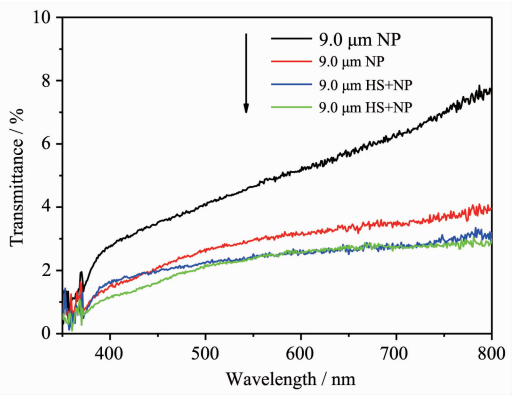

Fig.6　Transmission spectra of two kinds of electrode films with different thicknesses

scatters shows a great enhancement, either for a thickness of 6.5 μm or 9.0 μm. The improved light harvesting ability would lead to a larger photocurrent. As for the transmission spectra, the introduction of HSs leads to a significant decrease for a film of 6.5 μm, hence an increase of light harvesting. But as the film thickness increases to 9.0 μm, the use of HSs is not that effective. This is in good accordance with the *J-V* performances given above.

3　Conclusions

In summary, anatase TiO_2 nanosheet-based hierarchical spheres with nearly 100% exposed {001} facets were synthesized via a facile solvothermal process. The DSSCs composed of these hierarchical spheres as scatters were fabricated by electrophoresis deposition (EPD) method and show improved cell efficiency up to 7.66% owing to the enhanced dye adsorption and superior light harvesting ability.

References:

[1] O'Regan B C, Grätzel M. *Nature*, **1991**,**353**:737-740

[2] Yella A, Lee H W, Tsao H N, et al. *Science*, **2011**,**334**:629-634

[3] Tan B, Wu Y Y. *J. Phys. Chem. B*, **2006**,**110**:15932-15938

[4] Gratzel M. *Inorg. Chem.*, **2005**,**44**:6841-6851

[5] Hore S, Vetter C, Kern R, et al. *Sol. Energy Mater. Sol. Cells*, **2006**,**90**:1176-1188

[6] Yang W G, Wan F R , Chen Q W, et al. *J. Mater. Chem.*, **2010**,**20**:2870-2876

[7] Wei S, Feng G, Li G L, et al. *Chem. Commun.*, **2011**,**47**:5046-5048

[8] Zhu P, Nair A S, Yang S, et al. *J. Mater. Chem.*, **2011**,**21**:12210-12212

[9] Huang F, Chen D, Zhang X L, et al. *Adv. Funct. Mater.* **2010**,**20**:1-5

[10]Yang H G, Sun C H, Qiao S Z, et al. *Nature*, **2008**,**453**:638-U4

[11]Zhang D Q, Li G S, Yang X F, et al. *Chem. Commun.*, **2009**:4381-4383

[12]Liu G, Sun C, Yang H G, et al. *Chem. Commun.*, **2010**,**46**:755-757

[13]Chen J S, Tan Y L, Li C M, et al. *J. Am. Chem. Soc.*, **2010**, **132**:6124-6130

[14]Yang W, Li J, Wang Y, et al. *Chem. Commun.*, **2011**,**47**:1809-1811

[15]Matthews D, Kay A, Gratzel M, Aust. *J. Chem.*, **1994**,**47**:1869-1877

[16]Grinis L, Dor S, Ofir A, et al. *J. Photochem. Photobiol. A*, **2008**,**198**:52-59

[17]Park N G, Van de Lagemaat J, Frank A J, *J. Phys. Chem. B*, **2000**,**104**:8989-8994

[18]Lim B, Jiang M, Camargo P H C, et al. *Science*, **2009**,**324**:1302-1305

[19]Chen D, Huang F, Cheng Y B, et al. *Adv. Mater.*, **2009**,**21**:2206-2210

[20]Zhang H, Han Y, Liu X, et al. *Chem. Commun.*, **2010**,**46**:8395-8397